Defects in CoO in oxidized cobalt nanoparticles dominate exchange biasing and exhibit anomalous magnetic properties

Joseph B. Tracy and Moungi G. Bawendi*
Department of Chemistry, Massachusetts Institute of Technology, Cambridge, Massachusetts 02139, USA
(Received 3 April 2006; revised manuscript received 29 August 2006; published 30 November 2006)

Defects can vastly modify the optical, electrical, mechanical, and magnetic properties of materials. In this paper, we report an investigation of the magnetic properties of moments associated with defects in CoO in partially and fully oxidized colloidal Co nanoparticles. The defect moments freeze at low temperature and have a distribution of melting temperatures, in which most melt below 50 K, but exchange biasing (EB) generated by the CoO lattice stabilizes the Co core moments in the partially oxidized sample up to 170 K [J. B. Tracy, D. N. Weiss, D. P. Dinega, and M. G. Bawendi, Phys. Rev. B **72**, 064404 (2005)]. By switching the polarity of the biasing field at intermediate temperatures during cooling, we show that the defect moments dominate EB at low temperature and exhibit a thermal memory effect. Selected cooling sequences show that the exchange shift (H_{EB}) may change sign as the sample is heated and demonstrate tuning of H_{EB} and the coercivity. Thermal remanent magnetization measurements directly show how changes in the orientation of CoO defect moments cause the Co core moments to reorient. An investigation of the temporal stability of the defect moments is also reported.

DOI: 10.1103/PhysRevB.74.184434 PACS number(s): 75.75.+a, 81.07.−b

I. INTRODUCTION

There is currently great interest in preparing nanoparticles (NPs) of antiferromagnets (AFMs)[1–16] and ferromagnet (core)/AFM (shell) NPs for numerous applications. Interfaces between ferromagnets (FMs) and AFMs may exhibit an additional unidirectional anisotropy caused by magnetic coupling at the interface, which is called exchange biasing (EB). The interface between Co (FM) and CoO (AFM) has been used as a prototype for studying EB because it has a large unidirectional anisotropy, and the ordering temperature of bulk CoO, the Néel temperature (T_N), is near room temperature at 293 K.[17] When Co(core)/CoO(shell) NPs[1,18–29] with a sufficiently thick[30] core and shell are cooled in a magnetic field, they exhibit EB. For further background on EB, we refer to recent reviews.[31–35]

Uncompensated moments (UCMs) have been observed in thin films of CoO.[17,36,37] These UCMs can be classified as one of two types: (1) Some UCMs are strongly exchange coupled to the AFM lattice, and have T_N near to that of the rest of the AFM lattice. (2) Other UCMs are weakly exchange coupled to the AFM lattice and become paramagnetic at much lower temperatures than the lattice.[17,36] The weak coupling of these UCMs to the AFM lattice may be caused by spin frustration, especially along grain boundaries, or where there are crystal or stoichiometric defects, and they may exhibit spin glasslike behavior.[36,38–41] In this work, we show that UCMs with weak coupling to the AFM lattice dominate EB in Co(core)/CoO(shell) NPs at low temperature.

Since the initial discovery of EB in oxidized Co NPs,[18] many models have been proposed, but a comprehensive microscopic understanding of EB remains lacking. It has been well established that spins at FM/AFM interfaces adopt an orthogonal arrangement which is known as "spin-flop coupling,"[42] but such an arrangement is possible without giving rise to EB.[43] EB depends on the crystallographic and magnetic domain structure of the AFM,[44–47] and roughened FM/AFM interfaces may exhibit enhanced[48] or reduced EB[33] compared with smooth ones.

Central to recent models of EB is the magnetic domain structures of both the AFM and FM. Because the Co cores in our NPs are single domain and too small to sustain domain walls,[31] we consider only AFM domains. Grain boundaries and defects can stabilize domain walls in the AFM,[44,49] which are thought to cause EB through one of two mechanisms:[47,50] (1) AFM domain walls couple to and pin the FM core.[46,47,51,52] (2) Moments at the FM/AFM interface couple to and pin the core.[53] However, defects induced away from the FM/AFM interface can aid the formation of domain walls and thereby modify the domain structure, including the interfacial moments, which control EB.[44,45,54–56] Others have attributed the pinning to a spin glasslike phase, which is similar to (2).[38,44] Geometry is also important, and FM(core)/AFM(shell) NPs have been investigated computationally.[57,58]

Here, we present a comprehensive study of moments associated with crystal defects at surfaces and grain boundaries and stoichiometric defects, which are caused by variations in the Co to O ratio, in the CoO shell of partially and fully oxidized colloidal Co NPs. At least a portion of these defect moments are UCMs that are weakly coupled to the AFM lattice, and they have a critical role in EB. This work is a continuation of our recent investigation of EB in partially oxidized Co NPs, in which we observed defect moments in thin ($t \sim 3$ nm) CoO shells in partially and fully oxidized Co NPs.[1] At low temperature, magnetization (M) vs field (H) for fully oxidized NPs after field cooling in a 5 T field exhibits a superparamagnetic component and has a vertical shift along the magnetization axis, which we attributed to the defect moments.

We proceed after the experimental section (Sec. II) by introducing M vs H measurements in which the polarity of the biasing field was switched during cooling (Sec. III A). Using these switching procedures, the exchange shift (H_{EB})

and the coercivity (H_C) can be tuned, H_{EB} can be caused to change sign as the sample is heated, and the defect moments are shown to dominate over EB generated by the CoO lattice at low temperature. In the following section (Sec. III B), data from thermal remanent magnetization (TRM) measurements after switching during cooling are used to demonstrate a thermal memory effect and to observe the distribution of defect moment melting temperatures. A correlation of the temperature- and field-dependent data for fully oxidized CoO (Sec. III C) is then presented, followed by an investigation of the temporal stability of the defect moments (Sec. III D) and a discussion of additional data with cooling to 2.5 K (Sec. III E).

II. EXPERIMENT

The samples investigated here are the same set that we studied previously.[1] We refer to Ref. 1 for the procedures to prepare, oxidize, and incorporate the NPs into polymer sticks. After preparing one batch of NPs using colloidal chemistry methods, portions were oxidized in solution to different extents: (1) The NPs in the "native" sample have an average Co core of diameter 7.2 nm with a CoO shell that is 1.0 nm thick. (2) The "partial" sample was purposefully oxidized by exposing the NP solution to air at room temperature. The partially oxidized NPs have an average Co core of diameter 3.3 nm and a CoO shell of thickness 3.2 nm. (3) By bubbling air through a solution of the NPs at elevated temperature, the NPs in "full" sample were fully oxidized to CoO, and hollow cavities formed where the cores had been.[1]

For superconducting quantum interference device (SQUID) measurements, the NPs were dispersed in dilute concentrations into a polymer with average interparticle distances of greater than 70 nm, so that dipolar coupling between NPs would be negligible.[59] These NP/polymer samples were stored in a nitrogen glove box in order to prevent further oxidation. Elemental analysis for Co was performed on the polymer samples by Galbraith Laboratories, Inc., using inductively coupled plasma—optical emission spectroscopy.

SQUID measurements were performed on a Quantum Design MPMS-5S. In the M vs H measurements, a correction was performed to remove the diamagnetic background of the polymer. The magnetization units of emu/g reported throughout this paper are based on the mass of cobalt. The mass of ligands and oxygen in the oxidized samples is excluded.

III. RESULTS AND DISCUSSION

We precede the discussion of magnetic measurements by addressing some potential concerns about our samples. One concern is the effects of the size distributions of ferromagnetic cores and antiferromagnetic grains. In exchange biased systems, the EB blocking temperature is defined as the temperature at which H_{EB} becomes zero, but for ferromagnetic NPs, the superparamagnetic blocking temperature is the temperature at which the ferromagnetic moments have lost their orientation and become superparamagnetic. Throughout this paper, when we discuss the blocking temperature (T_B) without further specification, it is the temperature at which the ferromagnetic core becomes superparamagnetic, and T_B is enhanced by EB.[1,19] The EB blocking temperature is related to T_B, but we do not measure it directly. For ferromagnetic NPs without EB, the size distribution causes a distribution of T_B.[60,61] The CoO shell on our native sample is too thin to cause EB,[1,19,30] and the size distribution is 7.8 ± 1.0 nm, which propagates into $T_B = 120 \pm 43$ K.[1] This size distribution does lead to broadening in our temperature-dependent data for the native sample, in which magnetocrystalline anisotropy is the predominant magnetic effect, but this does not restrict our interpretation of the data.

The temperature-dependent data of the partial sample, however, is controlled by EB. Variations in the AFM, such as grain size and orientation, are known to lead to a distribution of EB blocking temperatures,[62–68] which has also been observed in thin films of exchange biased CoO.[36,69] One size-dependent mechanism by which an AFM grain may no longer pin a FM is if the AFM grain becomes superparamagnetic.[1,22] The distribution of EB blocking temperatures should cause a corresponding distribution in T_B for an exchange biased superparamagnet.

In the partial sample, some variation in the grain size and orientation, and therefore in the EB blocking temperature for each AFM grain is expected. The M vs T data [Ref. 1, and reproduced in Fig. 5(b)] show a distinct peak at 170 K, which may be broadened by a distribution of the EB blocking temperatures. However, the low-temperature rise in the zero field cooled (ZFC) M vs T (predominantly below 50 K) is distinctly separate and does not result from broadening of the peak at 170 K. For this reason, the variation among the AFM grains does not impede our analysis, and we assign the low-temperature rise to defect moments.

Another concern about ferromagnetic NPs is the effect of interparticle coupling. Dipolar coupling between ferromagnetic NPs causes T_B to increase, and can also change the coercivity.[59] In our samples, the interparticle coupling is negligible because the NPs are diluted in a polymer. Moreover, oxidation of the NP core reduces the strength of the dipolar coupling.

A. Role of defects in exchange biasing

In the following experiment, we exploited the different thermal stabilities of EB generated by (1) the CoO lattice and any UCMs that are tightly coupled to it, which we call the "lattice," and (2) UCMs that are weakly coupled to the AFM, which we call "defect moments," because they are associated with grain boundaries, surfaces, and stoichiometric impurities. When a defect moment "melts," it is no longer able to maintain its orientation. The lattice causes EB in the partial sample up to 170 K, but the defect moments melt at lower temperatures, as evidenced by a low temperature rise in the M vs T measurements.[1] Recently, others have observed a similar low-temperature rise in M vs T for CoO NPs.[2,3,6,8] In order to separate the effects of EB due to the lattice and the defect moments, at different temperatures, the cooling field was switched to the opposite polarity or to zero field.[70,71] Melted defect moments were reoriented by the switched

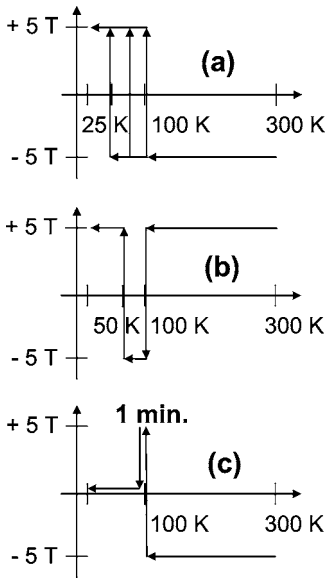

FIG. 1. Cooling procedures for the (a) first, (b) second, and (c) third switching experiments.

field, but frozen defect moments and the lattice moments could not be reoriented.

The procedures for switching during field cooling are presented in Fig. 1. Each M vs H measurement was performed on both the partial and full samples. The magnetization data were analyzed according to the following procedure, which we developed in Ref. 1: The magnetization of the partial sample has components caused by the exchange biased core and the susceptibility of CoO. After subtracting the magnetization of the full sample, which was scaled to account for the fact that the partial sample was not fully oxidized, the magnetization of the exchange biased core is $M_{partial} - 0.947 M_{full}$. Each M vs H curve was fit in order to remove the superparamagnetic signal from small clusters of unoxidized Co in the diffusion zone between the core and shell, and the values for H_{EB} and H_C (Fig. 2, insets) were taken from the curve fitting.

In the first switching experiment, the partial and full samples were cooled in a −5 T field from room temperature to an intermediate switching temperature (T_{switch}) of 25, 50, or 100 K, at which the biasing field was switched to 5 T before resuming cooling to 5 K. This cooling procedure is depicted in Fig. 1(a), and the corresponding data are in Fig 2(a). By cooling to below 170 K in a −5 T field, the lattice is frozen to pin the Co cores along the negative field direction, but some defect moments reorient and pin the core in the positive field direction upon further cooling.

For T_{switch} of 25 K, $H_{EB,5\ K} = -0.34$ T. For comparison, after field cooling to 5 K in a −5 T field, $H_{EB,5\ K} = -0.70$ T.[1] As T_{switch} was increased to 50 K, $H_{EB,5\ K} = -0.10$ T. For $T_{switch} = 100$ K, at 5 K, $H_{EB,5\ K} = 0.36$ T, and then after heating to 100 K in a 5 T field and measuring again, $H_{EB,100\ K} = -0.13$ T. Therefore, for $T_{switch} = 100$ K, H_{EB} has changed sign during the heating process. By heating the sample up to 100 K, the defect moments that were frozen below 100 K have melted, and they can no longer pin the core. These results are consistent with a distribution of defect moment

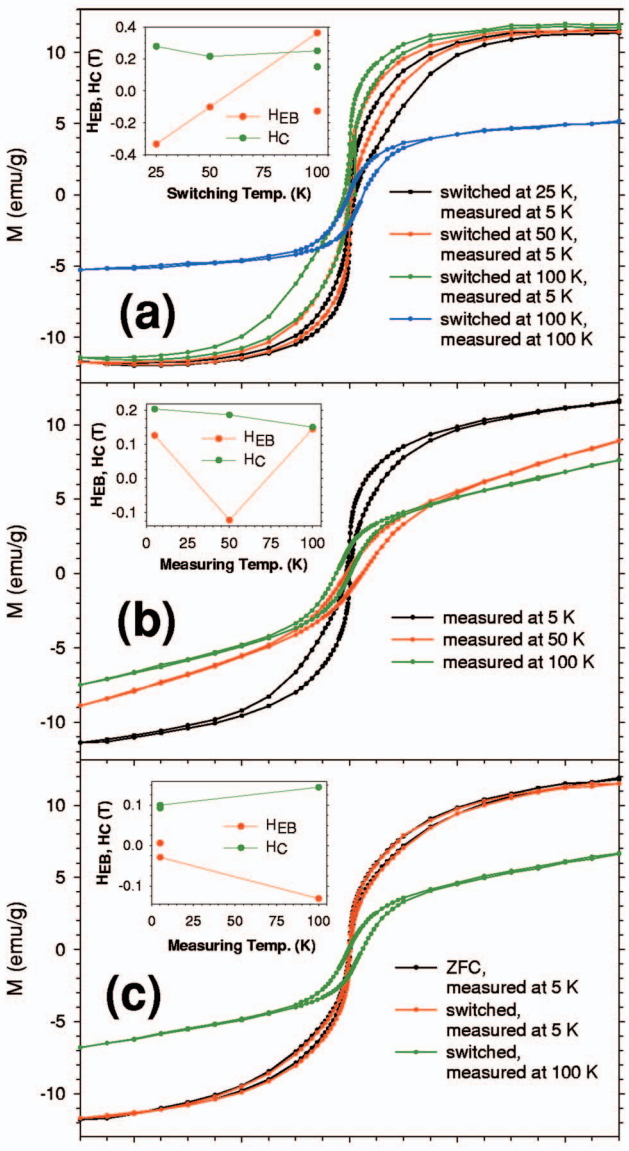

FIG. 2. (Color) Measurements at 5 K, 50 K and 100 K of ($M_{partial} - 0.947\ M_{full}$) vs H after cooling from 300 K: (a) in a −5 T field, followed by switching to 5 T at 25 K, 50 K, or 100 K and resuming cooling to 5 K; (b) to 100 K in a 5 T field, from 100 K to 50 K in a −5 T field, and from 50 K to 5 K in a 5 T field; (c) to 100 K in a −5 T field, then switching to 5 T for 1 min and cooling to 5 K in zero field; compared with the zero field cooled curve measured at 5 K. Insets (a-c): H_{EB} and H_C vs T from the fit for each curve.

freezing temperatures below 170 K, and switching at higher temperatures allows more defect moments to reorient, which causes H_{EB} to increase.

In the second switching experiment [Figs. 1(b) and 2(b)], the biasing field was switched twice during cooling, and H_{EB} changed sign twice during heating. The partial and full samples were cooled to 100 K in a 5 T field. At 100 K, the field was switched to −5 T, and cooling was resumed to 50 K, where the field was switched to 5 T, and cooling was continued to 5 K. This double change in the sign of H_{EB} is further evidence that the defect moments have a distribution

of freezing temperatures. The defect moments which froze in the negative field direction between 50 K and 100 K dominate EB at 50 K, because the defect moments which were frozen below 50 K have melted, thus causing $H_{EB,50\ K}<0$. If the defect moments were all to have the same freezing temperature rather than a distribution of freezing temperatures, a maximum of one sign change of H_{EB} would be possible, because the defects could dominate at low temperature and the lattice could dominate at high temperature, but it would be impossible to freeze portions of the defect moments in opposite directions according to their freezing temperatures.

These switching experiments also show that switching may be used to tune the value H_{EB}. Other investigations have shown that EB can be tuned by using different strengths of cooling fields[72–76] or by preparing the FM with different remanent magnetizations at $T>T_N$ and then cooling in zero field,[77] and EB may be randomized by cooling in an ac field.[70,71] In our third switching experiment [Figs. 1(c) and 2(c)], the cooling procedure randomizes EB at 5 K: The partial and full samples were cooled to 100 K in a −5 T field. At 100 K, the field was switched to 5 T for one min, and then to zero field before resuming cooling to 5 K. M vs H was measured at 5 K, and then again after heating to 100 K. For comparison, the samples were cooled to 5 K in zero field and were measured at 5 K.

The overlap between the switched and the ZFC curves measured at 5 K is remarkable. When the fitting procedure was applied to the switched curve, $H_{C,5\ K}=0.100$ T and $H_{EB,5\ K}=-0.029$ T, and for the ZFC curve, $H_{C,5\ K,ZFC}=0.093$ T and $H_{EB,5\ K,ZFC}=0.0058$ T, which serves as an estimate of the error in the fitting procedure. At 5 K, H_{EB} and H_C for the switched and ZFC curves are quite similar. Following the measurement at 5 K, the switched sample was heated to 100 K and M vs H was measured again, for which $H_{EB,100\ K}=-0.13$ T. Therefore, at 100 K, EB is no longer randomized. We lack a complete understanding of how the randomization occurs at 5 K but not at 100 K, but the following is a plausible: Upon switching at 100 K, the defect moments which are not already frozen switch into the positive field direction. After switching to zero field, some of these defect moments have a nonzero H_C and continue pinning in the positive direction, in which they freeze during further cooling. After cooling to 5 K, the pinning effects of the lattice and defect moments in the negative field direction cancel out with the pinning effects of the defect moments in the positive field direction, but at 100 K, only the lattice and defect moments that froze above 100 K continue pinning the core in the negative field direction.

In both the first and third switching experiments, H_{EB} can be tuned to values which are near zero. We now compare M vs H from the first (for $T_{switch}=50$ K) and third switching experiments. In the first experiment, $H_{C,switch50\ K}=0.22$ T $>H_{C,thirdexperiment}=0.10$ T. Although H_{EB} is reduced in both cases, the coercivities and the shapes of the curves differ substantially. In both measurements, EB caused by the lattice and defect moments that freeze above T_{switch} nearly cancels out with the EB generated by the defect moments that freeze below T_{switch}. However, in the first experiment, switching occurs at a lower temperature (50 K, rather than 100 K). Therefore, the EB generated by the lattice and defect moments that freeze above T_{switch} should be greater in the first experiment. We similarly expect the EB generated by the defect moments below T_{switch} in the first experiment to be greater than in the third experiment, because those in the first experiment were cooled in a 5 T field rather than zero field. Thus, the magnitudes of exchange bias that nearly cancel out in the first experiment are greater than those which nearly cancel out in the third experiment. Therefore, H_C can be tuned at least partially independently of H_{EB} by using the principle that H_C has a greater enhancement from two opposing effects of greater magnitude that give rise to EB than from two smaller opposing effects.[74]

B. Thermal remanent magnetization and memory effect

In the following measurements, we observed the distribution of defect moment melting temperatures and a thermal memory effect using TRM measurements, in which the sample was cooled in a field to low temperature and then measured in zero applied field during heating. A thermal memory effect requires a distribution of blocking temperatures, such that during cooling, part of the system may be reoriented after another part has frozen. This has been observed for both (1) ferromagnetic NPs, in which the size distribution causes a distribution of T_B,[78–81] and (2) for exchange biased systems, in which the EB blocking temperature has a distribution.[70,82]

TRM measurements of the full sample after cooling to 5 K in fixed fields of 0.1, 1, and 5 T are presented in Fig. 3(d). Further measurements in another SQUID magnetometer with 7 T field cooling overlap with the curve at 5 T. Therefore, a field of 5 T is required to orient most of the defect moments during cooling, which is indicative of frustrated spins. This result contrasts with some thin film studies, in which EB is essentially independent of cooling field, except for small ($\ll 1$ T) fields.[45,83]

In order to observe the distribution of melting temperatures and thermal memory effect, TRM measurements (Fig. 3) for the native, partial, and full NPs were performed after cooling to T_{switch} in a −5 T field, and then switching to 5 T and resuming cooling to 5 K, which is the same cooling procedure as in our first switching experiment [Fig. 1(a)]. For the measurement identified as TRM, the sample was cooled to 5 K in a 5 T field without switching. (Similar measurements of the remanent magnetization for the cooling procedure used in the second switching experiment [Fig. 1(b)] are presented and discussed in the supporting information,[84] Fig. SI-2.)

The magnetization curves (Fig. 3) show that the native sample has no memory of switching, but the partial and full samples do. Because the CoO shell on the native NPs is too thin to cause EB,[1,19,30] the core moments were saturated in the 5 T field that was applied immediately before measurement. The low-temperature rise in the remanent magnetization for the partial and full samples is similar to that of M vs T in a small applied field.[1] During heating and measurement, the magnetization initially decreases as defect moments that were frozen in the positive field direction melt. At 5–10 K above T_{switch}, the defect moments which were frozen in the

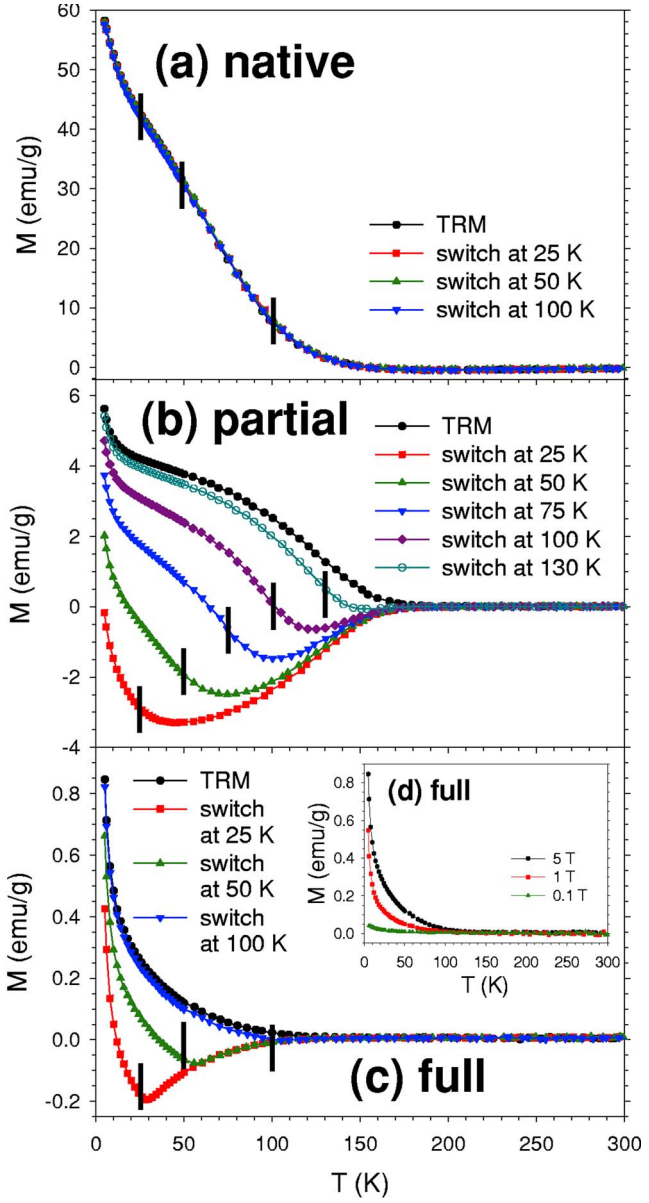

FIG. 3. (Color online) TRM and remanent magnetization after cooling from 300 K in a −5 T field, followed by switching to 5 T at a variety of temperatures (indicated by black bars) for (a) native, (b) partial, and (c) full oxidation; and (d) TRM of the full sample with different cooling fields: 0.1 T, 1 T, and 5 T.

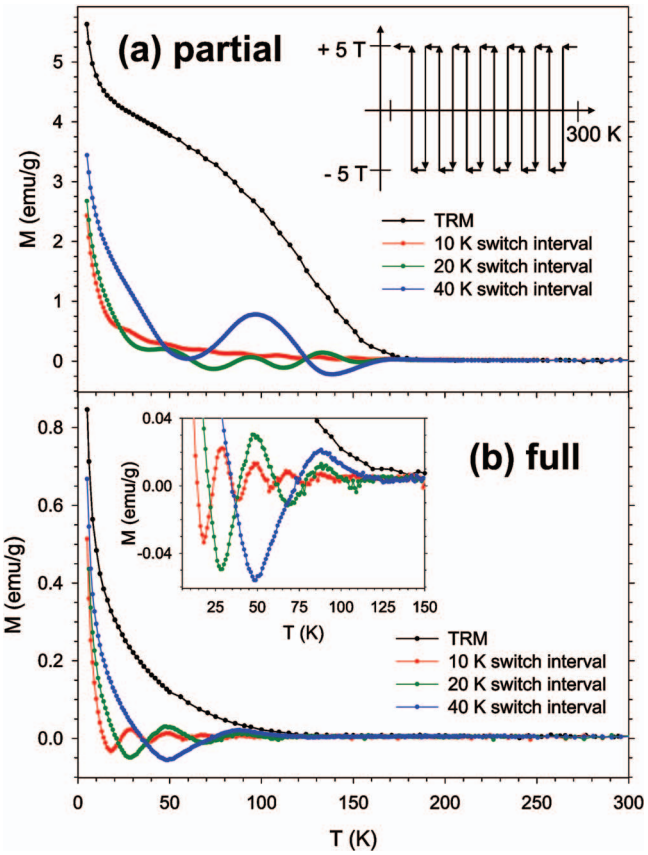

FIG. 4. (Color) TRM and remanent magnetization after cooling from 300 K in a ±5 T field switched at intervals of 10 K, 20 K, or 40 K during cooling for (a) partial and (b) full oxidation; inset is an expansion of the low temperature region for the full sample.

negative field direction begin to melt, and the magnetization increases towards zero. For the partial sample, the effects of EB on the magnetization of the cores are also observed. Because $M_{TRM,partial,5\ K}=5.6$ emu/g, and $M_{TRM,full,5\ K}=0.85$ emu/g, we approximate that about 5 emu/g of the magnetization in the partial sample is caused by the cores. We attribute the low-temperature cusp in the TRM for the partial sample to the magnetization of the defect moments in the shell, because the cusp is about 1 emu/g high and has the same steep rise as for the full sample. The minimum in the magnetization for the partial sample occurs at a temperature that is 20–40 K higher than T_{switch}. This additional temperature delay for reversing the orientation of the core moment implies that more thermal energy is required for the core moments to change orientations as the pinning caused by the defects in the shells changes.

The relative effects of the lattice and defect moments on EB can be observed by comparing the remanent magnetization curves with $T_{switch}=100$ K for the full and partial samples. For the full sample, this curve nearly overlaps the unswitched TRM, which implies that most defect moments have melted below 100 K. The UCMs that are strongly coupled to the lattice and melt at 170 K are not significantly observed, and we expect that they sum to zero magnetization, because of the spherical geometry of the polycrystalline AFM shell and averaging over many NPs. For the partial sample, a significant difference remains between the $T_{switch}=100$ K curve and the TRM, which is caused primarily by the lattice, and by the few defect moments with melting temperatures greater than 100 K.

The thermal memory effect is most pronounced when the TRM is measured after switching between ±5 T at regular temperature intervals of 10 K, 20 K, and 40 K during cooling to 5 K (Fig. 4). For each measurement, the last temperature interval ending at 5 K was chosen to be in 5 T field. The full sample remembers each field inversion with high precision, and the memory in the partial sample has less precision in temperature, because of the larger increase in temperature above T_{switch}, is needed in order for the core to reorient into the new pinning environment created by the defects.

Important questions remain: What is the switching behavior of a single NP, and how does summing over multiple NPs give the ensemble behavior observed here? How uniformly are the defect moments distributed among the NPs? The number of possible switching events in a single NP would be limited by the number of independent defect moments and their distribution of melting temperatures. In order to address these questions, single NP magnetometry would be necessary.

The measurements of the full sample clearly show that the defect moments in CoO can be reoriented and frozen according to their freezing temperatures. Therefore, the TRM curve corresponding to cooling in an unswitched 5 T field is a measure of the total number of frozen defect moments at a particular temperature. The derivative, $-dM_{TRM}/dT$ (Fig. 5) thus gives the melting temperature distribution for the defect moments. The ZFC M vs T curves measured in 0.01 T field are also plotted, to which $-dM_{TRM}/dT$ has been scaled by multiplying by 3.39 for the partial sample and 3.63 for the full sample. The scaling factor 21.0 was used for the native sample. However, in contrast to the case for the partial and full samples, for the native sample, the maxima do not occur at 5 K for both the ZFC M vs T and $-dM_{TRM}/dT$.

The overlap between the two curves for the full sample is rather unexpected. (Additional measurements of the ZFC M vs T were taken down to 2.5 K, and the overlap breaks down below 5 K. These data are presented and discussed in Sec. III E.) The TRM measurement involves cooling in a large field and measuring in zero field, but the ZFC M vs T is cooled in zero field and measured in a small field. However, the derivative of the TRM measurement can be reconciled with the ZFC M vs T curve if, in the latter, each defect moment orients in the field as it melts, but then becomes paramagnetic and quickly decays to nearly zero magnetization at a slightly higher temperature, thereby causing the ZFC M vs T curve to also give a distribution of the defect moments' melting temperatures.

The factors used to scale $-dM_{TRM}/dT$ to the ZFC M vs T curves for the partial and full samples are quite similar. The overlap between those curves for the partial sample is also good at low temperature, as would be expected, because that low-temperature rise has the same physical origin as for the full sample. However, at higher temperatures, the peaks in the ZFC M vs T curves that correspond to the blocking behavior of the core have little, if any, overlap with the derivative of the TRM curve, because these peaks do not originate from the melting of CoO defect moments.

In order to learn more about the freezing behavior and reorientation of defect moments and the cores via EB during heating, we carried out a series of TRM experiments using the cooling procedure in the third switching experiment [Fig. 1(c)] and variations thereof. Two additional experiments were performed on the native, partial, and full samples with a variety of switching temperatures (Fig. 6). In the first additional experiment, each sample was cooled in a 5 T field to T_{switch}, followed by cooling in zero field to 5 K. (Measurements of M vs H for this cooling procedure are presented and discussed in the supporting information,[84] Fig. SI-1). The same cooling procedure was used for the second additional experiment for the partial and full samples, except the field was switched to −5 T for 1 min at T_{switch} before switching to zero field and resuming cooling. For the native sample, the field polarities in the second additional experiment were reversed; it was cooled in a −5 T field to T_{switch}, where the field was switched to 5 T for 1 min, and then to zero field before resuming cooling to 5 K. TRM curves with constant 5 T field cooling and data for cooling in a ±5 T field to T_{switch} and then in the opposite field (green curves) are shown for comparison. (The latter are also shown in Fig. 3, but those for the partial and full samples are now inverted about the field axis.)

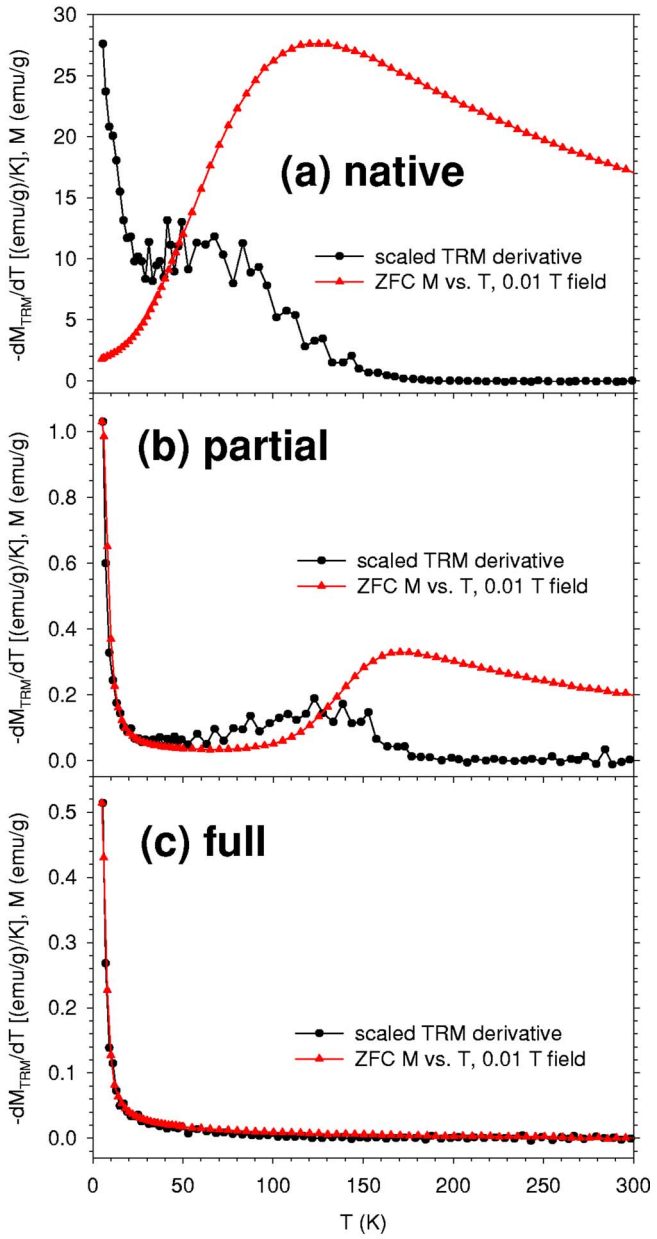

FIG. 5. (Color online) Scaled $-dM_{TRM}/dT$ and ZFC M vs T, measured in 0.01 T field for (a) native, (b) partial, and (c) full oxidation.

For each sample, the magnetization is nearly constant over the temperature range in which it was cooled in zero field. In the native sample, this remanent magnetization was

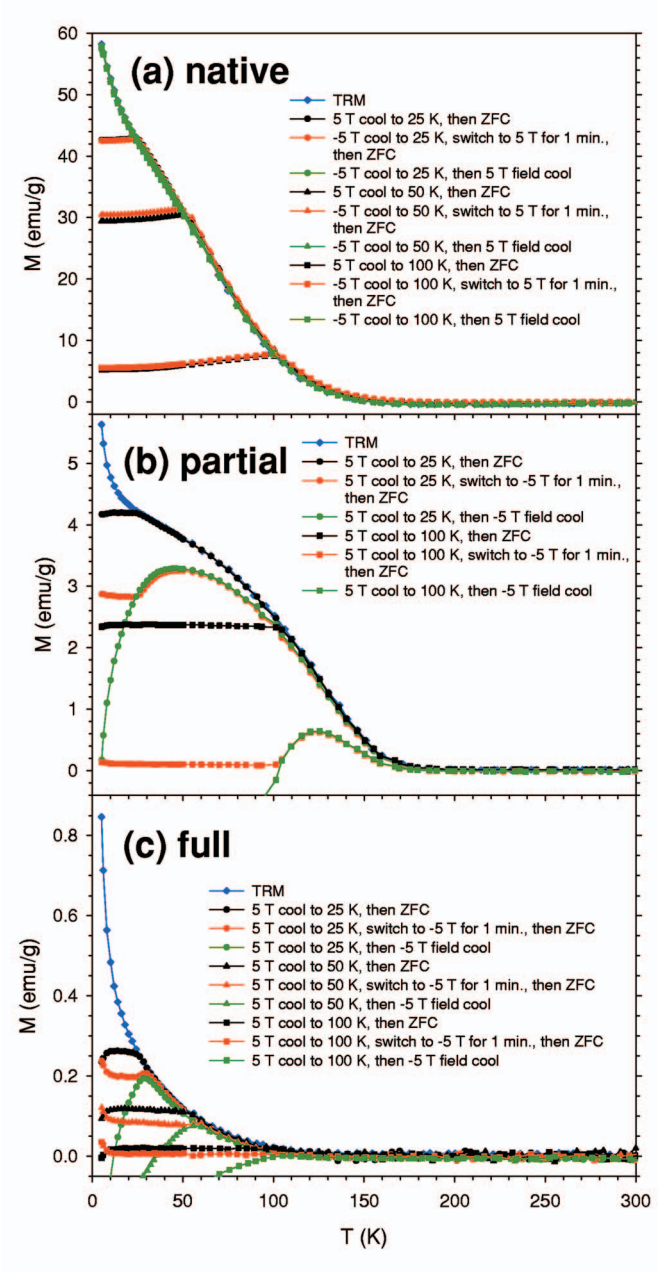

FIG. 6. (Color) TRM and remanent magnetization after cooling from 300 K in a ±5 T field to T_{switch}, where the field was switched either to zero field, to ±5 T for one min and then to zero field, or to ±5 T, and then cooling to 5 K for (a) native, (b) partial, and (c) full oxidation.

determined by the last switch to 5 T prior to switching to zero field and resuming cooling. (The data with switching at 50 K are reproducible, and it is not clear why the two curves with zero field cooling below 50 K do not overlap more closely.) For the full sample, however, the remanent magnetization was determined primarily by the initial cooling field of 5 T, in which the defect moments were frozen. The partial sample exhibited a more complicated behavior, which we discuss momentarily.

We now elucidate a more detailed understanding of the freezing process by comparing measurements of the full

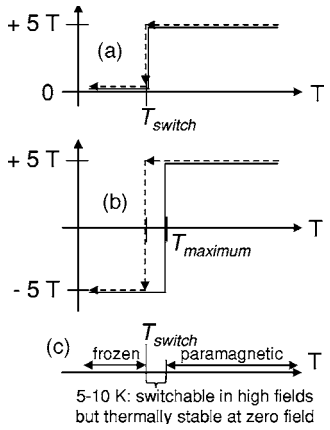

FIG. 7. Cooling procedures (dotted arrows) and schematics of the corresponding orientations, in which additional defect moments in the CoO shell (solid lines) freeze at each temperature for switching to (a) zero field and (b) opposite field; (c) summary of CoO defect moment melting behavior.

sample with and without the switch to −5 T for 1 min before resuming cooling at zero field [black and red curves in Fig. 6(c)]. The remanent magnetization was lower in the experiment with the 1 min switch to −5 T, which implies that some of the defect moments were reoriented and frozen into the negative field direction. Moreover, for T_{switch} of 25 K and 50 K, the curve without switching to −5 T for 1 min merges into the TRM curve at T_{switch} or the next data point above T_{switch}, but the curve with switching to −5 T for 1 min merges into the TRM curve at 5–10 K above T_{switch}. (The signal for the curves with T_{switch}=100 K is too small to readily identify such points.) Therefore, when the field is switched into the opposite direction, the defect moments with melting temperatures within 5–10 K above T_{switch} can be reoriented into the direction of the switched field. However, when the field is switched to zero, the defect moments with melting temperatures within 5–10 K above T_{switch} remain oriented in the direction of the previous cooling field. This last result is described schematically in Fig. 7. Procedures with switching to zero field and to the opposite field are depicted by the dashed arrows, and the solid line represents the direction in which the defect moments freeze at each temperature.

The partial sample [Fig. 6(b)] exhibits similar behavior to the full sample, except the magnetization of the Co core and its coupling to the CoO shell through EB are also observed. The curves with switching to zero field (black and red) at 25 K and 100 K merge at approximately 80 K above T_{switch}, because increased thermal energy is required to reorient the core moments as the pinning caused by the defects in the shells changes. However, the curves for the partial sample with switching to zero field have cusps at T_{switch} or at the next data point above T_{switch}, and those without switching to −5 T for 1 min merge into the TRM curve at this temperature. The curves for switching to −5 T for 1 min before zero field cooling (red curves) merge into the curves representing switching to and cooling in a −5 T field (green curves). Therefore, when the partial sample is heated after switching to zero field, no additional thermal energy is needed to

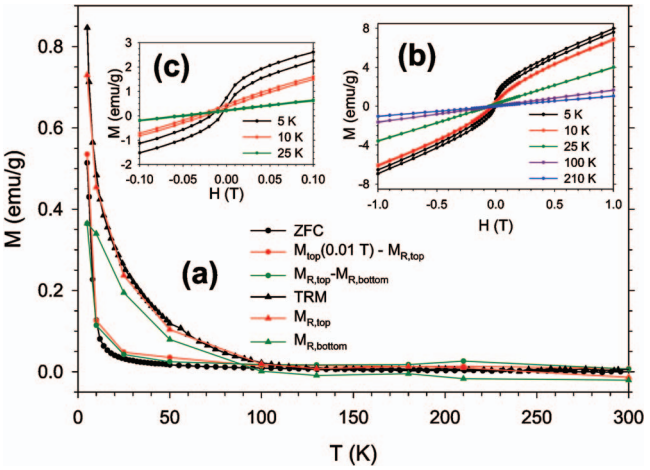

FIG. 8. (Color) Full sample: (a) calculations from the 5 T field cooled M vs H of $M_{R,top}$, $M_{R,bottom}$, $M_{R,top}-M_{R,bottom}$, and $M_{top}(0.01\ \mathrm{T})-M_{R,top}$, plotted with measurements of ZFC M vs T (0.01 T field) and TRM (5 T cooling) for comparison; (b) and (c) additional 5 T field cooled M vs H data to that in Ref. 1.

change the orientation of each core as the pinning environment of the defects in each shell changes, because the cores remain in their remanent magnetization state from before the field was switched off. The broad peaks, such as in Fig. 3(b), and the larger temperature delay for reorientation are only observed when an opposing field has been applied in the switching procedure during cooling.

The data in Fig. 6 also provide a greater understanding of M vs H in the third switching experiment [Fig. 2(c)]. The remanent magnetizations for the partial and full samples that were switched from 5 T to −5 T for 1 min at 100 K and then to zero field are both nearly zero, which is consistent with the small H_{EB} of M vs H at 5 K and its good overlap with the ZFC curve. The fourth switching experiment (supporting information,[84] Fig. SI-1) shows that switching to the opposite field for 1 min is required for overlap with the ZFC curve. The remanent magnetization measurements of the partial sample in Fig. 6(b) for switching to zero field at 100 K with and without the switch to −5 T for 1 min beforehand differ substantially.

C. Correlation of field- and temperature-dependent measurements

In Ref. 1, we observed that M vs H for the full sample with 5 T cooling has a small positive shift along the magnetization axis and a superparamagnetic component at low temperature. At low temperature, M vs H also exhibits hysteresis ($H_{C,5\ \mathrm{K}}=0.006$ T). Others have also observed hysteresis in CoO NPs at low temperature.[3,6,8] Our ZFC M vs T and TRM measurements correlate well with field cooled (FC) M vs H and enable further interpretation of its features. Additional M vs H data for the full sample cooled in a 5 T field and scanned between ±5 T are shown for fields around the origin in Figs. 8(b) and 8(c). From these data, we have computed and plotted [Fig. 8(a)] the remanence from the top ($M_{R,top}$) and bottom ($M_{R,bottom}$) curves of the hysteresis, $M_{R,top}-M_{R,bottom}$, and $M_{top}(0.01\ \mathrm{T})-M_{R,top}$. For comparison, the ZFC M vs T (0.01 T field) and TRM data (5 T cooling) are also shown.

As expected, $M_{R,top}$ overlaps with the TRM measurement, because both were cooled in 5 T fields. The quantity, $M_{top}(0.01\ \mathrm{T})-M_{R,top}$, correlates well with the ZFC M vs T (0.01 T field). As discussed earlier, the ZFC M vs T measurement shows CoO defect moments as they orient in the field when they melt, which is also measured in $M_{top}(0.01\ \mathrm{T})-M_{R,top}$. This correlation is not adversely affected by the different cooling fields of 5 T for M vs H and zero field for ZFC M vs T. The $M_{R,top}-M_{R,bottom}$ values correlate well with the ZFC M vs T (0.01 T field) data even though they are unscaled, which is unexpected, because the magnitude of the ZFC M vs T data should depend on the applied field, and 0.01 T was an arbitrary choice.

Three types of defect moments are observed in the 5 T field cooled M vs H measurements of the full sample at low temperature: (1) ($H_C>5$ T) Moments which are frozen and are not reoriented when the field is switched to −5 T, cause the vertical shift. (2) ($0<H_C<5$ T) The correlation between $M_{R,top}-M_{R,bottom}$ and the ZFC M vs T suggests that the hysteresis in M vs H has the same cause as the low-temperature rise in the ZFC M vs T; these defect moments are sufficiently molten that they can be reoriented in fields less than 5 T, but smaller fields are insufficient to reorient these defect moments. (3) ($H_C=0$) The superparamagnetic component most prevalent at low temperature in M vs H is caused by defect moments that will switch in any field but still interact significantly with their surroundings and are not yet paramagnetic.

D. Temporal stability

We present a detailed study of the temporal stability of the defect moments and exchange biased cores in the partial and full samples, along with a brief study of magnetic training, in the supporting information.[84] The main conclusion is that two relaxation processes occur that are observable on the time scale of SQUID measurements: In the full sample, there is a single energy barrier, $E_{a1}\approx 26\ k_BT$. In the partial sample, there are two energy barriers, the same $E_{a1}\approx 26\ k_BT$, and a larger barrier, $E_{a2}\approx 29\ k_BT$, which causes a component of the relaxation to be slower. This larger second barrier is consistent with our observation that after switching the field between ±5 T during cooling, the extrema in remanent magnetization measurements of the partial sample occur at temperatures significantly above T_{switch}. However, the magnitude of the E_{a1} fast relaxation in the partial sample is too large to be assigned solely to the defects, and therefore also involves core relaxation. The specific mechanisms that give rise to two energy barriers remain undetermined.

E. Data to 2.5 K

A recent paper reports results of EB in oxidized ε-Co NPs that differ significantly from our data. Bao *et al.* observed a peak at 8 K in the ZFC M vs T for their fully oxidized sample,[27] which prompted us to measure additional data for

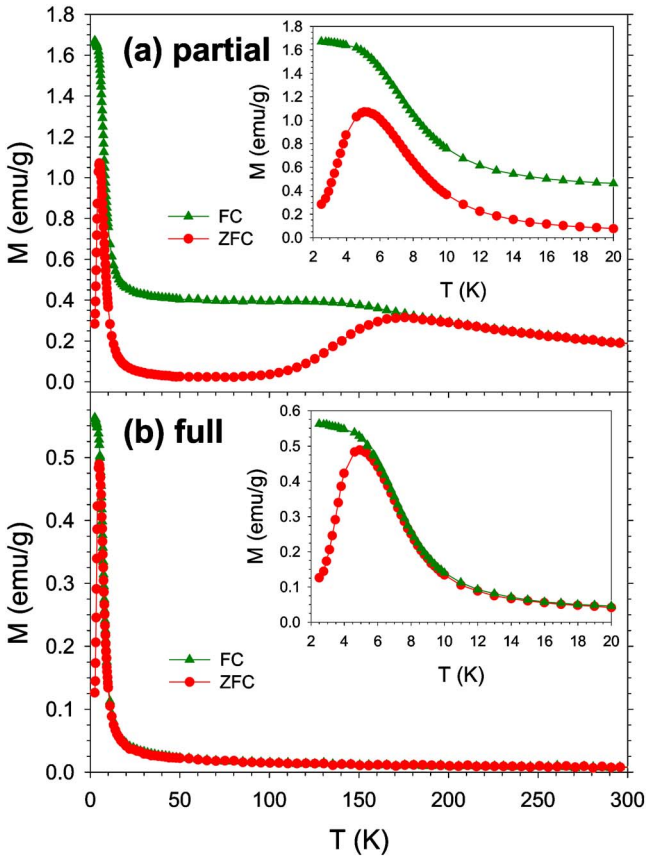

FIG. 9. (Color online) M vs T: FC (0.01 T) and ZFC, cooled to 2.5 K, measured in 0.01 T field for (a) partially and (b) fully oxidized samples. Insets show greater detail of the same measurements.

the partial and full samples to 2.5 K. FC and ZFC M vs T data were measured while heating the samples in a 0.01 T field (Fig. 9). Measurements of the TRM to 2.5 K using a −5 T cooling field for each sample are shown in the supporting information, in Fig. SI-8.[84]

The results are unexpected: The ZFC M vs T data for the partial and full samples have a peak at 5 K that we had not previously observed. For the full sample, the FC curve bifurcates from the ZFC curve at about 6 K and does not continue rising as sharply below 5 K as above it. We have already established that at temperatures above 5–6 K, the ZFC M vs T curve represents the distribution of the defect moment melting temperatures, because each defect moment melts and aligns into the field at its melting temperature, above which the magnetization quickly decays. Below 5 K, the physical picture changes: beginning at 2.5 K, the 0.01 T field is too weak to orient molten defect moments, and as the temperature is increased to 5 K, thermal energy assists the defect moments at aligning in the field. Therefore, the peak in the ZFC M vs T and the plateau in the FC M vs T curve at low temperature are caused by this requirement for increased thermal energy to orient molten defect moments in a 0.01 T field below 5 K.

In contrast, the TRM data grow much steeper below 5 K. Therefore, the distribution of the defect moment freezing temperatures continues increasing below 5 K. Many defects quickly lose their orientation and melt at $T<5$ K. The correlation between the derivative of the TRM and the ZFC M vs T curve for the partial and full samples breaks down below 5 K, because the TRM measurement can observe melting below 5 K, but the ZFC M vs T cannot.

IV. CONCLUSIONS

These experiments, in which the biasing field was switched during cooling, have yielded significant understanding of the magnetic properties of defects in Co NPs that have been fully oxidized to CoO and of how these defects affect EB in partially oxidized Co NPs. Although the CoO defects are only a small part of the composition of the partially oxidized NPs, the defects dominate the magnetic properties. The CoO defect moments have a distribution of melting temperatures, which enables unexpected phenomena, including a thermal memory effect and tuning of H_{EB} and H_C. EB is observed in the loop shift in M vs H, but TRM measurements directly show that changes in the orientations of defect moments in the fully oxidized sample are correlated with changes in the orientations of the Co cores in the partially oxidized sample. The temperature-dependent data also help explain the features of the field cooled M vs H curves for the full sample—a vertical shift, hysteresis, and a superparamagnetic component at low temperature—which should be general to AFM NPs that contain defects.

TRM measurements show that a defect moment at its freezing temperature with respect to thermal energy at zero field needs to be cooled another 5–10 K before it is fully pinned and can no longer be reoriented in a 5 T field. For the fully oxidized sample, the negative derivative of the TRM gives the distribution of melting temperatures of the defect moments, which correlates exceptionally well with the ZFC M vs T (0.01 T) for $T>5$ K, because the defect moments can orient in the 0.01 T field only in this 5–10 K window at their melting points, in which they are not fully pinned but their orientations have not yet been randomized by thermal energy. Two energy barriers for reorientation are present in the partial sample, one of which is considerably larger than the single barrier for the full sample and causes a sluggish response of the core magnetization as pinning by the defect moments changes.

Although we have achieved a detailed understanding of defect moments in an ensemble of NPs, interesting questions remain: What is their behavior at the single NP level? How does the distribution of defect moments and their melting behaviors differ from one NP to another?

ACKNOWLEDGMENTS

We thank Dirk Weiss, Bob O'Handley, Young Lee, Yuping Bao, and Marc Kastner for helpful discussions, comments, and suggestions. We gratefully acknowledge Fangcheng Chou for training on the SQUID magnetometer. This work was supported by the NSF-NSEC at Harvard, the NSF-MRSEC at MIT, a NSF-NIRT grant, and the Packard Foundation. J.B.T. acknowledges support from the US DOD.

*Author to whom correspondence should be addressed.
[1] J. B. Tracy, D. N. Weiss, D. P. Dinega, and M. G. Bawendi, Phys. Rev. B **72**, 064404 (2005).
[2] W. S. Seo, J. H. Shim, S. J. Oh, E. K. Lee, N. H. Hur, and J. T. Park, J. Am. Chem. Soc. **127**, 6188 (2005).
[3] H. T. Zhang and X. H. Chen, Nanotechnology **16**, 2288 (2005).
[4] X. Sun, Y. W. Zhang, R. Si, and C. H. Yan, Small **1**, 1081 (2005).
[5] N. R. Jana, Y. F. Chen, and X. G. Peng, Chem. Mater. **16**, 3931 (2004).
[6] M. Ghosh, E. V. Sampathkumaran, and C. N. R. Rao, Chem. Mater. **17**, 2348 (2005).
[7] J. S. Yin and Z. L. Wang, Phys. Rev. Lett. **79**, 2570 (1997).
[8] L. Y. Zhang, D. S. Xue, and C. X. Gao, J. Magn. Magn. Mater. **267**, 111 (2003).
[9] L. Zhang and D. Xue, J. Mater. Sci. Lett. **21**, 1931 (2002).
[10] C. F. J. Flipse, C. B. Rouwelaar, and F. M. F. De Groot, Eur. Phys. J. D **9**, 479 (1999).
[11] L. Wang, K. Vu, A. Navrotsky, R. Stevens, B. F. Woodfield, and J. Boerio-Goates, Chem. Mater. **16**, 5394 (2004).
[12] G. P. Glaspell, P. W. Jagodzinski, and A. Manivannan, J. Phys. Chem. B **108**, 9604 (2004).
[13] L. Soriano, M. Abbate, A. Fernández, A. R. González-Elipe, F. Sirotti, and J. M. Sanz, J. Phys. Chem. B **103**, 6676 (1999).
[14] R. Xu and H. C. Zeng, J. Phys. Chem. B **107**, 926 (2003).
[15] S. A. Makhlouf, J. Magn. Magn. Mater. **246**, 184 (2002).
[16] S. R. Mishra, I. Dubenko, J. Losby, K. Ghosh, M. Khan, and N. Ali, J. Nanosci. Nanotechnol. **5**, 2076 (2005).
[17] K. Takano, R. H. Kodama, A. E. Berkowitz, W. Cao, and G. Thomas, Phys. Rev. Lett. **79**, 1130 (1997).
[18] W. H. Meiklejohn and C. P. Bean, Phys. Rev. **105**, 904 (1957).
[19] V. Skumryev, S. Stoyanov, Y. Zhang, G. Hadjipanayis, D. Givord, and J. Nogués, Nature (London) **423**, 850 (2003).
[20] D. L. Peng, K. Sumiyama, T. Hihara, S. Yamamuro, and T. J. Konno, Phys. Rev. B **61**, 3103 (2000).
[21] M. Verelst, T. O. Ely, C. Amiens, E. Snoeck, P. Lecante, A. Mosset, M. Respaud, J. M. Broto, and B. Chaudret, Chem. Mater. **11**, 2702 (1999).
[22] S. Gangopadhyay, G. C. Hadjipanayis, C. M. Sorensen, and K. J. Klabunde, J. Appl. Phys. **73**, 6964 (1993).
[23] R. Morel, A. Brenac, and C. Portemont, J. Appl. Phys. **95**, 3757 (2004).
[24] M. Spasova, U. Wiedwald, M. Farle, T. Radetic, U. Dahmen, M. Hilgendorff, and M. Giersig, J. Magn. Magn. Mater. **272–276**, 1508 (2004).
[25] G. H. Wen, R. K. Zheng, K. K. Fung, and X. X. Zhang, J. Magn. Magn. Mater. **270**, 407 (2004).
[26] P. Imperia, D. Schmitz, H. Maletta, N. S. Sobal, and M. Giersig, Phys. Rev. B **72**, 014448 (2005).
[27] Y. P. Bao, M. Beerman, A. B. Pakhomov, and K. M. Krishnan, J. Phys. Chem. B **109**, 7220 (2005).
[28] V. Schneider, A. Reinholdt, U. Kreibig, T. Weirich, G. Güntherodt, B. Beschoten, A. Tillmanns, H. Krenn, K. Rumpf, and P. Granitzer, Z. Phys. Chem. (Munich) **220**, 173 (2006).
[29] S. M. Zhou, D. Imhoff, K. Yu-Zhang, and Y. Leprince-Wang, Appl. Phys. A: Mater. Sci. Process. **81**, 115 (2005).
[30] A. N. Dobrynin, D. N. Ievlev, K. Temst, P. Lievens, J. Margueritat, J. Gonzalo, C. N. Afonso, S. Q. Zhou, A. Vantomme, E. Piscopiello, and G. Van Tendeloo, Appl. Phys. Lett. **87**, 012501 (2005).
[31] J. Nogués, J. Sort, V. Langlais, V. Skumryev, S. Suriñach, J. S. Muñoz, and M. D. Baró, Phys. Rep. **422**, 65 (2005).
[32] A. E. Berkowitz and K. Takano, J. Magn. Magn. Mater. **200**, 552 (1999).
[33] J. Nogués and I. K. Schuller, J. Magn. Magn. Mater. **192**, 203 (1999).
[34] M. Kiwi, J. Magn. Magn. Mater. **234**, 584 (2001).
[35] R. L. Stamps, J. Phys. D **33**, R247 (2000).
[36] Y. J. Tang, D. J. Smith, B. L. Zink, F. Hellman, and A. E. Berkowitz, Phys. Rev. B **67**, 054408 (2003).
[37] T. Ambrose and C. L. Chien, Phys. Rev. Lett. **76**, 1743 (1996).
[38] M. Gruyters, Phys. Rev. Lett. **95**, 077204 (2005).
[39] B. Martínez, X. Obradors, L. Balcells, A. Rouanet, and C. Monty, Phys. Rev. Lett. **80**, 181 (1998).
[40] R. H. Kodama, A. E. Berkowitz, E. J. McNiff, and S. Foner, Phys. Rev. Lett. **77**, 394 (1996).
[41] R. K. Zheng, G. H. Wen, K. K. Fung, and X. X. Zhang, Phys. Rev. B **69**, 214431 (2004).
[42] N. C. Koon, Phys. Rev. Lett. **78**, 4865 (1997).
[43] T. C. Schulthess and W. H. Butler, Phys. Rev. Lett. **81**, 4516 (1998).
[44] U. Nowak, K. D. Usadel, J. Keller, P. Miltényi, B. Beschoten, and G. Güntherodt, Phys. Rev. B **66**, 014430 (2002).
[45] J. Keller, P. Miltényi, B. Beschoten, G. Güntherodt, U. Nowak, and K. D. Usadel, Phys. Rev. B **66**, 014431 (2002).
[46] M. D. Stiles and R. D. McMichael, Phys. Rev. B **59**, 3722 (1999).
[47] D. Suess, M. Kirschner, T. Schrefl, J. Fidler, R. L. Stamps, and J. V. Kim, Phys. Rev. B **67**, 054419 (2003).
[48] T. J. Moran, J. M. Gallego, and I. K. Schuller, J. Appl. Phys. **78**, 1887 (1995).
[49] J. V. Kim and R. L. Stamps, Appl. Phys. Lett. **79**, 2785 (2001).
[50] A. Hoffmann, J. W. Seo, M. R. Fitzsimmons, H. Siegwart, J. Fompeyrine, J. P. Locquet, J. A. Dura, and C. F. Majkrzak, Phys. Rev. B **66**, 220406 (2002).
[51] J. V. Kim and R. L. Stamps, Phys. Rev. B **71**, 094405 (2005).
[52] M. D. Stiles and R. D. McMichael, Phys. Rev. B **60**, 12950 (1999).
[53] H. Ohldag, A. Scholl, F. Nolting, E. Arenholz, S. Maat, A. T. Young, M. Carey, and J. Stöhr, Phys. Rev. Lett. **91**, 017203 (2003).
[54] A. Misra, U. Nowak, and K. D. Usadel, J. Appl. Phys. **95**, 1357 (2004).
[55] M. R. Ghadimi, B. Beschoten, and G. Güntherodt, Appl. Phys. Lett. **87**, 261903 (2005).
[56] G. Scholten, K. D. Usadel, and U. Nowak, Phys. Rev. B **71**, 064413 (2005).
[57] E. Eftaxias and K. N. Trohidou, Phys. Rev. B **71**, 134406 (2005).
[58] Ò. Iglesias, X. Batlle, and A. Labarta, Phys. Rev. B **72**, 212401 (2005).
[59] B. L. Frankamp, A. K. Boal, M. T. Tuominen, and V. M. Rotello, J. Am. Chem. Soc. **127**, 9731 (2005).
[60] R. K. Zheng, H. W. Gu, and X. X. Zhang, Phys. Rev. Lett. **93**, 139702 (2004).
[61] M. Sasaki, P. E. Jönsson, H. Takayama, and P. Nordblad, Phys. Rev. Lett. **93**, 139701 (2004).
[62] S. Soeya, T. Imagawa, K. Mitsuoka, and S. Narishige, J. Appl. Phys. **76**, 5356 (1994).
[63] J. P. Nozières, S. Jaren, Y. B. Zhang, A. Zeltser, K. Pentek, and V. S. Speriosu, J. Appl. Phys. **87**, 3920 (2000).
[64] S. Brück, J. Sort, V. Baltz, S. Suriñach, J. S. Muñoz, B. Dieny, M.

D. Baró, and J. Nogués, Adv. Mater. (Weinheim, Ger.) **17**, 2978 (2005).
[65] M. Tsunoda, Y. Tsuchiya, M. Konoto, and M. Takahashi, J. Magn. Magn. Mater. **171**, 29 (1997).
[66] C. H. Lai, T. J. Regan, R. L. White, and T. C. Anthony, J. Appl. Phys. **81**, 3989 (1997).
[67] A. N. Dobrynin, D. N. Ievlev, C. Hendrich, K. Temst, P. Lievens, U. Hörmann, J. Verbeeck, G. Van Tendeloo, and A. Vantomme, Phys. Rev. B **73**, 245416 (2006).
[68] M. Grimsditch, A. Hoffmann, P. Vavassori, H. T. Shi, and D. Lederman, Phys. Rev. Lett. **90**, 257201 (2003).
[69] T. Ambrose and C. L. Chien, J. Appl. Phys. **83**, 6822 (1998).
[70] N. J. Gökemeijer, J. W. Cai, and C. L. Chien, Phys. Rev. B **60**, 3033 (1999).
[71] Y. F. Li, J. Q. Xiao, and D. V. Dimitrov, J. Appl. Phys. **91**, 7227 (2002).
[72] H. T. Shi, D. Lederman, N. R. Dilley, R. C. Black, J. Diedrichs, K. Jensen, and M. B. Simmonds, J. Appl. Phys. **93**, 8600 (2003).
[73] J. Nogués, D. Lederman, T. J. Moran, and I. K. Schuller, Phys. Rev. Lett. **76**, 4624 (1996).
[74] C. Leighton, J. Nogués, B. J. Jönsson-Åkerman, and I. K. Schuller, Phys. Rev. Lett. **84**, 3466 (2000).
[75] J. Nogués, L. Morellon, C. Leighton, M. R. Ibarra, and I. K. Schuller, Phys. Rev. B **61**, R6455 (2000).
[76] T. J. Moran and I. K. Schuller, J. Appl. Phys. **79**, 5109 (1996).
[77] P. Miltényi, M. Gierlings, M. Bamming, U. May, G. Güntherodt, J. Nogués, M. Gruyters, C. Leighton, and I. K. Schuller, Appl. Phys. Lett. **75**, 2304 (1999).
[78] M. Sasaki, P. E. Jönsson, H. Takayama, and H. Mamiya, Phys. Rev. B **71**, 104405 (2005).
[79] R. K. Zheng, H. W. Gu, B. Xu, and X. X. Zhang, Phys. Rev. B **72**, 014416 (2005).
[80] S. Chakraverty, M. Bandyopadhyay, S. Chatterjee, S. Dattagupta, A. Frydman, S. Sengupta, and P. A. Sreeram, Phys. Rev. B **71**, 054401 (2005).
[81] G. M. Tsoi, L. E. Wenger, U. Senaratne, R. J. Tackett, E. C. Buc, R. Naik, P. P. Vaishnava, and V. Naik, Phys. Rev. B **72**, 014445 (2005).
[82] Y. F. Li, R. H. Yu, J. Q. Xiao, and D. V. Dimitrov, J. Appl. Phys. **87**, 4951 (2000).
[83] T. Gredig, I. N. Krivorotov, P. Eames, and E. D. Dahlberg, Appl. Phys. Lett. **81**, 1270 (2002).
[84] See EPAPS Document No. E-PRBMDO-74-001642 for supporting information. This document can be reached via a direct link in the online article's HTML reference section or via the EPAPS homepage (http://www.aip.org/pubservs/epaps.html).